

# Infrapatellar fat pad features in osteoarthritis: a histopathological and molecular study

Marta Favero<sup>1,2</sup>, Hamza El-Hadi<sup>3</sup>, Elisa Belluzzi<sup>1</sup>, Marnie Granzotto<sup>3</sup>, Andrea Porzionato<sup>4</sup>, Gloria Sarasin<sup>4</sup>, Anna Rambaldo<sup>4</sup>, Claudio Iacobellis<sup>5</sup>, Augusto Cigolotti<sup>5</sup>, Chiara Giulia Fontanella<sup>6</sup>, Arturo Natali<sup>6</sup>, Roberta Ramonda<sup>1</sup>, Pietro Ruggieri<sup>5</sup>, Raffaele De Caro<sup>4</sup>, Roberto Vettor<sup>3</sup>, Marco Rossato<sup>3</sup> and Veronica Macchi<sup>4</sup>

## Abstract

**Objective.** The infrapatellar fat pad (IFP) is considered a local producer of adipocytokines, suggesting a potential role in OA. The objective of this study was to evaluate the histopathological and molecular characteristics of OA IFPs compared with controls.

**Methods.** The histopathological characteristics of IFPs were evaluated in patients undergoing total knee replacements and in control patients (without OA), considering the following parameters: presence of inflammatory cells, vascularization, adipose lobules dimension and thickness of the interlobular septa. Immunohistochemistry was performed to evaluate VEGF, monocyte chemotactic protein 1 (MCP-1) and IL-6 proteins. Quantitative real time PCR was performed to evaluate the expression levels of adipocytokines in the OA IFPs.

**Results.** OA IFPs showed an increase in inflammatory infiltration, vascularization and thickness of the interlobular septa compared with controls. VEGF, MCP-1 and IL-6 proteins were higher in OA IFPs compared with in controls. Inflammatory infiltration, hyperplasia, vascularization and fibrosis were increased in OA IFP synovial membranes compared with in those of controls. VEGF protein levels were associated with an increased number of vessels in the OA IFPs, while MCP-1 and IL-6 protein levels were associated with higher grades of inflammatory infiltration. Leptin levels were positively correlated with adiponectin and MCP-1 expression, while adiponectin positively correlated with peroxisome proliferative activated receptor gamma, MCP-1 and IFP vascularity. MCP-1 showed a positive correlation with peroxisome proliferative activated receptor gamma. IFP lobules dimensions were positively correlated with IL-6 expression and negatively with thickness of interlobular septa. VEGF mRNA levels were positively correlated with increased synovial vascularity.

**Conclusions:** OA IFPs and synovial membranes are more inflamed, vascularized and fibrous compared with those of control patients (without OA).

**Key words:** osteoarthritis, knee, infrapatellar fat pad, total knee replacement

<sup>1</sup>Rheumatology Unit, Department of Medicine – DIMED, University Hospital of Padova, Padova, <sup>2</sup>Laboratory of Immunorheumatology and Tissue Regeneration/RAMES, Rizzoli Orthopedic Research Institute, Bologna, <sup>3</sup>Department of Medicine – DIMED, School of Medicine, Clinica Medica 3, <sup>4</sup>Institute of Human Anatomy, Department of Neurosciences, University of Padova, <sup>5</sup>Orthopaedic Clinic, Department of Surgery, Oncology and Gastroenterology, University-Hospital of

Padova and <sup>6</sup>Centre for Mechanics of Biological Materials, University of Padova, Padova, Italy

Submitted 13 October 2016; revised version accepted 16 June 2017

Correspondence to: Marco Rossato, Department of Medicine – DIMED, School of Medicine, University of Padova, Clinica Medica 3, Via Giustiniani, 2, 35128 Padova, Italy.  
E-mail: marco.rossato@unipd.it

**Rheumatology key messages**

- The infrapatellar fat pad of osteoarthritic patients is characterized by increased lymphocytic infiltration, vascularization and thickness of septa.
- The adjacent synovial membrane of osteoarthritic patients showed increased fibrosis, lymphocytic infiltration, vascularization and hyperplasia.
- A possible cross-talk between the infrapatellar fat pad and the synovial membrane in OA is suggested.

**Introduction**

OA is the most common musculoskeletal disorder and a major cause of pain and disability in the adult population [1]. The knee is the main joint affected by OA [2], with a prevalence estimated between 10 and 13% in elderly people [3]. A novel concept considers OA as a whole-joint inflammatory disease, involving not only cartilage but also subchondral bone, meniscus and synovial membrane [4]. Inflammatory cytokines, chemokines and other inflammatory mediators are produced by synovium, cartilage, and other joint tissues and can be measured in the SFs of OA patients [5].

In the knee, the infrapatellar fat pad (IFP) is situated between the patellar tendon, femoral condyles and tibial plateau and located closely to the synovial layers and cartilage surfaces, where it can influence these structures [6]. Although the IFP was traditionally considered as having only a buffering and lubricating function, recent studies have shown that this tissue might be a local modulator of inflammatory responses contributing to the initiation and progression of knee OA [7, 8]. Similarly to other adipose depots, the IFP might be a source of pro-inflammatory cytokines, called adipokines, which have been largely found in the SF of OA patients [9]. The cytokine production/expression of the IFP has been investigated only in a few studies [10, 11]. In 2003 Ushiyama *et al.* [12] showed that homogenates of IFP tissue obtained from patients undergoing surgery expressed basic fibroblast growth factor, IL-6, VEGF and TNF- $\alpha$ . Furthermore, Distel *et al.* [10] found an increase in IL-6 and IL-6 soluble receptor secretion in the IFP of obese OA patients, suggesting a role for the IFP in OA inflammation. Finally, Klein-Wieringa *et al.* [11] characterized the immune cell fraction of the IFP, revealing a more inflammatory phenotype than that of the subcutaneous adipose tissue.

Although recent findings suggest a role for the IFP in the pathogenesis of OA, the actual contribution of the IFP to OA pathology is yet to be fully clarified. Histologically normal IFP consists of white adipose tissue, organized in lobules delimited by thin connective septa, rich in collagen I fibres [13].

The distinguishing microscopic and morphologic characteristics of the osteoarthritic IFP compared with those of the normal IFP have not yet been clearly described. Moreover, a microscopic scoring system for the OA IFP is not available. In the present study we evaluated the histopathological and molecular characteristics of the IFP of OA patients.

**Methods****Patients and tissue collection**

Twenty-eight patients fulfilling the ACR classification criteria for knee OA [14] and undergoing total knee replacement (TKR) for OA at the Orthopaedic Clinic of the University-Hospital of Padova (Italy) were enrolled in the study after providing written informed consent. The Ethical Committee of Padova Hospital approved the study, and the study was carried out in accordance with the principles of the Declaration of Helsinki. The following clinical data were collected: age, sex, BMI and comorbidities. During surgery, the IFP and adjacent synovial membrane were collected and processed as follows: an aliquot was fixed in 10% formalin and then paraffin-embedded for histochemical studies, and another was frozen in liquid nitrogen and stored at  $-80^{\circ}\text{C}$ .

The controls were represented by IFP and adjacent synovial membrane specimens sampled (at least 48 h post-mortem) from bodies or body parts of healthy subjects without history of symptomatic OA involved in the Body Donation Program known as Donation to Science (held by Padova University) [13]. The cadavers did not exhibit macroscopic evidence of OA.

**Microscopical study**

Thick sections of  $10\mu\text{m}$  were obtained from the paraffin-embedded samples, and were stained with haematoxylin-eosin (EE) or used for immunohistochemistry (IHC). We focused on the evaluation of both the IFP and the adjacent synovial membrane. The microscopical characteristics of the IFP were scored according to the presence of lymphocytic infiltration, vascularization, adipose lobules dimension and thickness of the interlobular septa. The presence of mononuclear cell infiltration was evaluated in EE-stained tissue sections and graded as follows: grade 0 = no presence of lymphocytic infiltration; grade 1 = presence of perivascular mononuclear cell infiltration; grade 2 = both perivascular and interstitial mononuclear cell infiltration.

Vascularization was evaluated in the EE-stained tissue sections, counting the number of vessels in the whole slice in four slices for each case. The mean number of vessels was considered.

The synovial membrane involvement was evaluated according to a synovial histopathological grading [15, 16] considering lymphocytic infiltration (0–3), synovial hyperplasia (0–2), vascularization (0–2), fibrosis (0–2), mucoid change (0–4) and detritus (0–2).

The grading characteristics were independently scored by two authors (V.M. and A.P.), using a DM4500-B light microscope (Leica Microsystems, Wetzlar, Germany) and recorded in full colour (24-bit) with a digital camera (DFC 480, Leica Microsystems). The intra- and inter- reliability of IFP lymphocytic infiltration were 0.92 and 0.91, respectively. Inter- and intra-rater reliability of synovial membrane histological features ranged between 0.92 and 1.

### Morphometry

After digitizing the images acquired from EE-stained sections, the diameter of the adipocyte lobuli and the thickness of the interlobular septa were measured, using specific imaging software (Adobe Photoshop CS5, Adobe Systems Incorporated, USA). Septa were first manually identified in the images acquired at  $\times 1.25$  primary magnification. Then, using a specific Programming Language Software (Matlab R2012b, The MathWorks, Inc., USA), images were converted to 8-bit binary images. The thickness of interlobular septa and the dimensions of adipose lobuli were then evaluated.

### IHC

Immunohistochemical stains were performed in IFPs as follows: anti-VEGF antibody (polyclonal mouse antibody, Santa Cruz Biotechnology); anti-monocyte chemotactic protein 1 (MCP-1) (polyclonal rabbit antibody, Thermo Fisher); anti-IL-6 antibody (polyclonal mouse antibody, Thermo Fisher). The anti-VEGF antibody was used with a dilution of 1:200 and antigen retrieval with proteinase K; the anti-MCP-1 antibody was used with a dilution of a 1:200 without antigen retrieval; and the anti-IL-6 antibody was used with a dilution of 1:200 without antigen retrieval. The sections were incubated using the DAKO Autostainer System (EnVision™ FLEX, High pH). Sections incubated without primary antibody showed no immunoreactivity, confirming the specificity of the immunostaining.

Vascularization evaluated by IHC with anti-VEGF was graded as follows: 1: <20 vessels labelled; 2: 20–40 vessels labelled; and 3: >40 vessels labelled. The localization of MCP-1 and IL-6 was evaluated by IHC on stained tissue sections using the following score: grade 0: no presence of cell staining; grade 1: presence of positive isolated roundish cells; grade 2: presence of both positive isolated roundish cells and crown-like structures, as previously reported [17].

### Quantitative real-time PCR

Total RNA was extracted from IFP not in contact with synovial membrane using a QIAMP mini kit (QIAGEN), following the manufacturer's protocol. First-strand cDNAs were synthesized from equal amounts of total RNA using random primers and M-MLV reverse transcriptase (Promega). Quantitative real time PCR (qRT-PCR) for adipokines [leptin, adiponectin, peroxisome proliferative activated receptor gamma2 (PPAR), fatty acid binding protein 4], cytokines (IL-6, TNF- $\alpha$ , MCP-1), VEGF and TGF- $\beta$  was performed using SYBR Green fluorophore.

Reaction efficiency was established for each set of primers and for an endogenous unregulated reference gene (18S) (after quantification of six different dilutions of the cDNA pool) and calculated from the slope according to the equation  $E = 10^{-1/\text{slope}}$  [18]. The cycle threshold (Ct) for each sample was used to calculate the amount of selected candidate and reference mRNAs relative to the internal standard. Relative quantification was based on the expression of the target gene toward the 18S rRNA housekeeping gene giving a ratio of the gene of interest. Real-time PCR was performed in triplicate for each gene and carried out in duplicate for each sample by DNA Engine Opticon 2 (MJ Research, Waltham, MA, USA). Post PCR analysis (Melting Curve) confirmed the specificity of the amplification signal target of our gene. Sequences of primers are reported in supplementary Table S1, available at *Rheumatology* Online. It was not possible to extract mRNA from the IFPs of cadavers for technical reasons since the bodies were available to the Anatomy Department at least 48 h after the death, resulting in mRNA degradation.

### Statistical analysis

Inter- and intra-reader reliability of histopathology scores were reported as a weighted kappa statistic. The Shapiro-Wilk test was used to determine whether data were distributed normally. The data were shown as means (s.d.). The chi-square test or Fisher's exact test was performed to compare categorical and dichotomous data. The Mann-Whitney test or Student's *t* test were used to compare continuous variables. Spearman's or Pearson's correlations were performed to analyse associations between continuous variables. One-way analysis of variance or the Kruskal-Wallis test, with Tukey's *post hoc* tests, was used to analyse categorical data. A  $P < 0.05$  was considered as statistically significant. All analyses were performed with SPSS version 22.0.

## Results

### Patient demographic and clinical characteristics

Twenty-eight patients undergoing TKR for OA were enrolled in the study. Specimens were also collected from eight cadavers as controls (without OA) (Table 1). There were 75% females in the OA group and 50% in the control group ( $P = 0.047$ ). OA subjects were statistically younger ( $P < 0.0001$ ) than the controls. BMI was statistically higher ( $P = 0.0002$ ) in the OA patients than in the controls.

### IFP histology, IHC and morphometry

Twenty-seven IFP samples underwent histologic and morphologic analysis (one sample was not analysed for technical reasons). The IFPs showed typical microscopical characteristics of white adipose tissue organized in adipose lobuli separated by fibrous septa (Fig. 1). The IFP histological characteristics are summarized in Table 2. No differences were detected in the mean diameter of OA IFP adipose lobuli compared with those of controls. The vascularity (evaluated in both EE-stained and



**TABLE 1** Demographic and clinical data of OA patients and controls

	OA patients	Controls	P-value
Number of patients	28	8	
Sex, female, <i>n</i> (%)	21 (75)	4 (50)	0.047*
Age, mean (s.d.), years	68.9 (7.8)	81.8 (4.9)	<0.0001*
BMI, mean (s.d.), kg/m <sup>2</sup>	30.5 (5.0)	21.8 (2.3)	0.0002*
Comorbidities			
Hypertension, <i>n</i> (%)	17 (68)	6 (60)	0.382
Diabetes, <i>n</i> (%)	3 (12)	3 (30)	0.073
Hypercholesterolaemia, <i>n</i> (%)	8 (32)	3 (30)	0.468

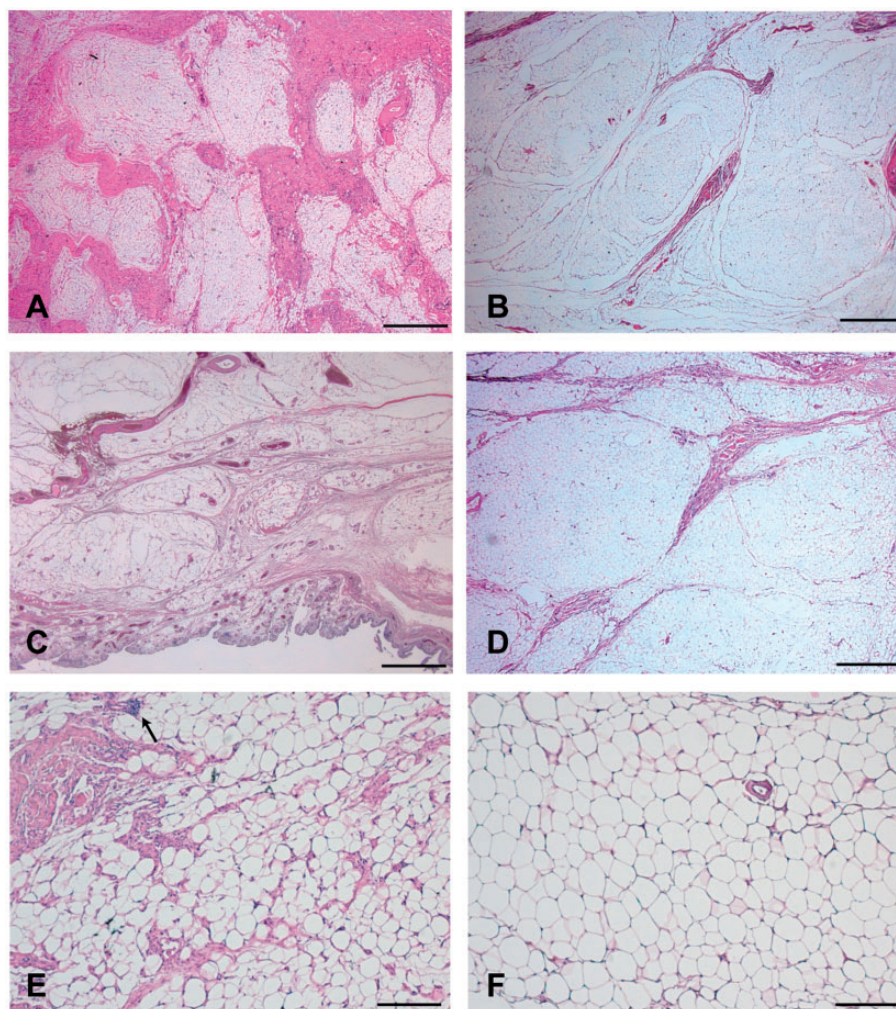
\* $P < 0.05$ .

anti-VEGF-stained sections), and the thickness of the interlobular septa was significantly higher in OA patients compared with in controls ( $P < 0.0001$  and  $P = 0.004$ , respectively) (Figs 1 and 2). Lymphocytic infiltration was present in 22 OA patients (81.5%), while it was not observed in any of the IFPs used as controls ( $P = 0.001$ ).

OA patients with presence of IFP lymphocytic infiltration had thicker lobuli septa ( $P = 0.055$ ) and smaller adipose lobuli ( $P = 0.040$ ) compared with OA subjects without IFP lymphocytic infiltration. The percentage of IL-6- and MCP-1-positive roundish cells and/or crown-like structures were significantly higher in the OA IFP patients compared with in the controls ( $P < 0.0001$ ) (Table 2 and Fig. 2).

#### Synovial membrane histopathological characteristics

The synovial membrane involvement was evaluated in 22 cases. The presence of lymphocytic infiltration and

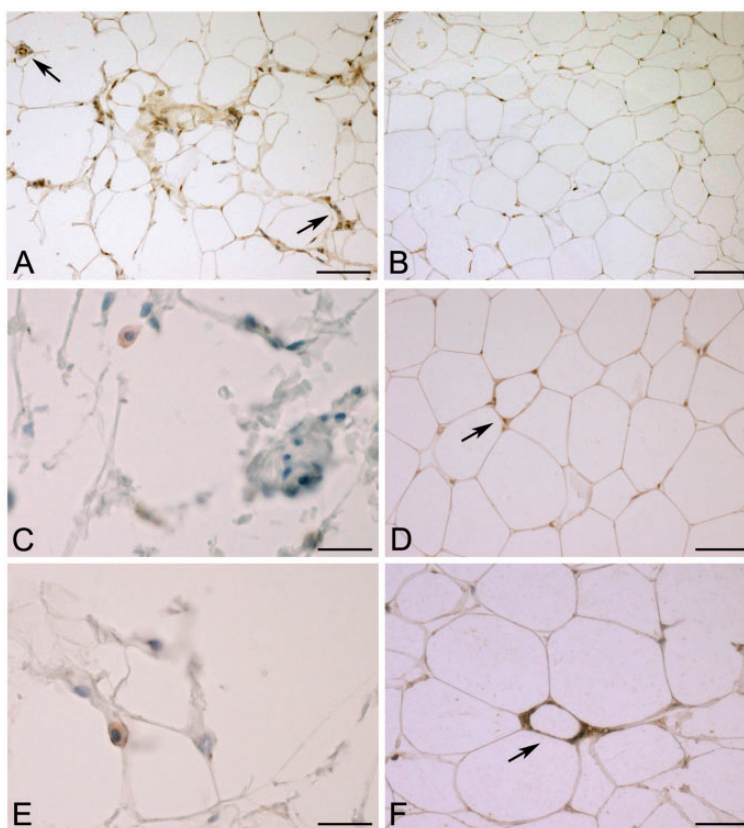
**Fig. 1** Histological features of infrapatellar fat in OA and in control

Microscopic appearance of the IFP in OA (left column) and in control (right column), showing the adipose lobuli separated by thick fibrous septa in OA (A) compared with in the controls (B). In OA patients the vessels were more numerous (C) with compared with in the controls (D), and showed major mononuclear infiltration (highlighted by the arrow) (E) compared with in the controls (F). A–F, haematoxylin-eosin. Scale bars: (A–D), 600  $\mu$ m; (E and F), 150  $\mu$ m.

**TABLE 2** Infrapatellar fat pad histopathologic and immunohistochemistry scoring system

IFP histopathologic grading	OA patients ( <i>n</i> = 27)	Controls ( <i>n</i> = 8)	<i>P</i> -value
Lymphocytic infiltration, <i>n</i> (%)			0.001*
Grade 0	5 (18.5)	8 (100)	
Grade 1	8 (29.6)	0 (0)	
Grade 2	14 (51.9)	0 (0)	
Vascularity in EE, number, mean (s.d.)	34.91 (16.26)	11.81 (4.25)	<0.0001*
Thickness of the interlobular septa, mean (s.d.), mm	0.30 (0.08)	0.23 (0.03)	0.004*
Diameter of adipose lobuli, mean (s.d.), mm	1.09 (0.42)	1.15 (0.11)	0.141
IFP immunohistochemistry grading			
VEGF, <i>n</i> (%)			<0.0001*
Grade 1	5 (18.5)	8 (100)	
Grade 2	12 (44.4)	0 (0)	
Grade 3	10 (37.1)	0 (0)	
MCP-1, <i>n</i> (%)			<0.0001*
Grade 0	0 (0)	6 (80)	
Grade 1	12 (44.4)	2 (20)	
Grade 2	15 (55.6)	0 (0)	
IL-6, <i>n</i> (%)			<0.0001*
Grade 0	0 (0)	6 (80)	
Grade 1	14 (51.9)	2 (20)	
Grade 2	13 (48.1)	0 (0)	

\**P* < 0.05. IFP: infrapatellar fat pad; EE: haematoxylin–eosin; MCP-1: monocyte chemotactic protein 1.

**FIG. 2** Immunohistochemistry features of OA infrapatellar fat pad

Vascularity evaluated by VEGF immunostaining of OA IFPs (**A**) and controls (**B**). IL-6 immunostaining of OA patients, showing the presence of isolated roundish cells with positive cytoplasm in the context of the IFP (**C**) and forming crown-like structures (**D**). MCP-1 immunostaining of OA patient, showing the presence of isolated roundish cells with positive cytoplasm in the context of the IFP (**E**) and forming crown-like structures (**F**). Scale bars: **A** and **B** = 75 µm; **C** and **E** = 23.8 µm; **D** and **F** = 37.5 µm.

**TABLE 3** Synovitis score of synovial membrane adjacent to infrapatellar fat pad

Synovitis histopathologic grading	OA patients (n = 22)	Control (n = 8)	P-value
Lymphocytic infiltration (0–3)			<0.001*
Grade 0	0 (0)	6 (75)	
Grade 1	5 (22.7)	2 (25)	
Grade 2	6 (27.2)	0 (0)	
Grade 3	11 (50)	0 (0)	
Vascularity (0–2)			<0.001*
Grade 0	0 (0)	8 (100)	
Grade 1	6 (27.3)	0 (0)	
Grade 2	16 (72.7)	0 (0)	
Detritus (0–2)			0.545
Grade 0	19 (86.4)	8 (100)	
Grade 1	2 (9.1)	0 (0)	
Grade 2	1 (4.5)	0 (0)	
Fibrosis (0–2)			0.002*
Grade 0	4 (18.2)	7 (87.5)	
Grade 1	10 (45.5)	1 (12.5)	
Grade 2	8 (36.4)	0 (0)	
Hyperplasia (0–2)			0.001*
Grade 0	3 (13.6)	7 (87.5)	
Grade 1	10 (45.5)	1 (12.5)	
Grade 2	9 (40.9)	0 (0)	
Mucoid change (0–4)			0.277
Grade 0	16 (72.7)	7 (87.5)	
Grade 1	0 (0)	1 (12.5)	
Grade 2	3 (13.6)	0 (0)	
Grade 3	1 (4.5)	0 (0)	
Grade 4	2 (9.1)	0 (0)	

\*Data are expressed as n (%).  $P < 0.05$ .

hyperplasia was statistically higher in the OA synovial membrane compared with that of controls ( $P < 0.001$ ,  $P = 0.001$ , respectively). In addition, the synovial membrane of OA patients was more vascularized and fibrotic compared with that of controls ( $P < 0.001$ ,  $P = 0.002$ , respectively). No differences were found in mucoid change and detritus between OA patients and controls. The histological characteristics of the IFP adjacent synovial membrane are described in detail in Table 3 and Fig. 3.

#### qRT-PCR analysis

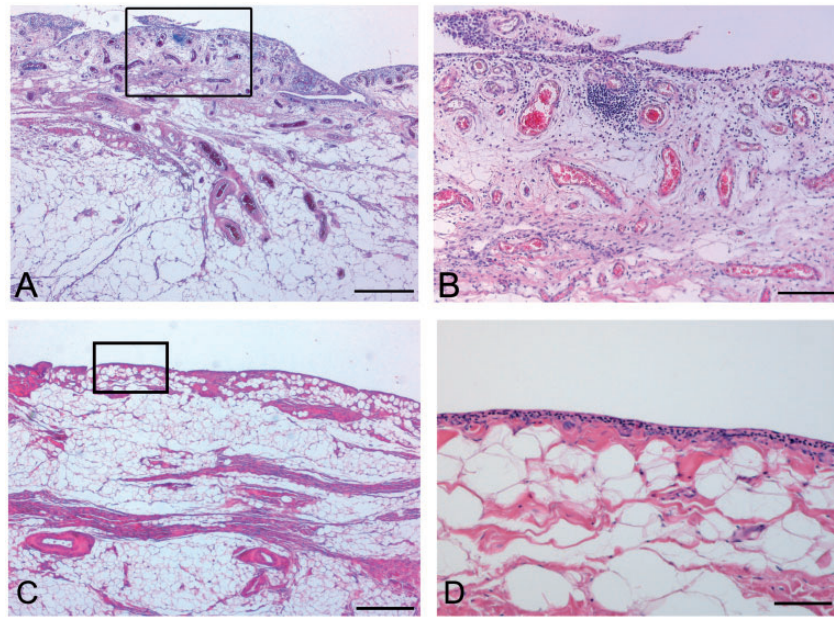
We analysed 26 IFP OA samples (two samples were not suitable for the molecular analysis for technical reason). All analysed samples showed the expression of white adipose tissue typical genes (leptin, adiponectin, PPAR $\gamma$  and fatty acid binding protein 4), inflammatory markers (IL-6, TNF $\alpha$  and MCP-1), markers of neoangiogenesis (VEGF) and fibrosis (TGF- $\beta$ ). Since it was not possible to evaluate the molecular profile of cadaver IFPs, gene expression levels of OA IFPs were correlated with clinical (age and BMI) and histological characteristics. In particular, gene expression levels were not found to differ between patients with or without lymphocytic infiltration in the IFP or in the adjacent synovial membrane. In addition, the molecular expression profile was not statistically different

between overweight ( $25 > \text{BMI} < 30$ ) or obese ( $\text{BMI} \geq 30$ ) patients compared with that of normal-weight subjects.

#### Correlations between gene expression levels, clinical and histological data

In OA IFPs, expression levels of leptin mRNA showed a positive correlation with those of adiponectin ( $P < 0.001$ ,  $r = 0.876$ ) and MCP-1 ( $P = 0.017$ ,  $r = 0.462$ ), and the expression of adiponectin positively correlated with that of PPAR $\gamma$  ( $P < 0.001$ ,  $r = 0.940$ ) and MCP-1 ( $P = 0.003$ ,  $r = 0.564$ ). Moreover, a strong positive correlation was found between MCP-1 and PPAR $\gamma$  gene expression levels ( $P < 0.001$ ,  $r = 0.903$ ). Notably, adiponectin mRNA expression levels were positively correlated with BMI ( $P = 0.035$ ;  $r = 0.415$ ) and the number of blood vessels of OA IFPs ( $P = 0.021$ ,  $r = 0.458$ ). The OA IFP lobules dimensions were positively correlated with IL-6 gene expression ( $P = 0.002$ ,  $r = 0.599$ ) and negatively correlated with the thickness of interlobular septa ( $P = 0.039$ ,  $r = -0.399$ ). BMI was positively correlated with the thickness of interlobular septa ( $P = 0.032$ ,  $r = 0.414$ ). IFP VEGF mRNA expression levels were positively correlated with increased synovial vascularity ( $P = 0.04$ ). VEGF protein levels detected by IHC were associated with a higher number of vessels as detected in EE sections of the OA IFPs ( $P < 0.0001$ ), while MCP-1 and IL-6 immunostainings of



**Fig. 3** Histological features of infrapatellar fat pad adjacent synovial membrane

Microscopic appearances of the IFP adjacent synovial membrane in OA (first row) and in control patients (second row), showing the presence of lymphocytic infiltration of the synovial membrane (**A** and **B**) compared with in the control (**C** and **D**). In OA patients the vessels were more numerous (**B**). (**A–D**), haematoxylin–eosin. Scale bars: **A** and **C** = 600  $\mu\text{m}$ ; **B** and **D** = 150  $\mu\text{m}$ .

OA IFPs were associated with higher grades of lymphocytic infiltration as evaluated in EE sections ( $P < 0.0001$ ). In addition, higher OA IFP IL-6 scores evaluated by IHC were associated with higher grades of synovial membrane fibrosis evaluated in EE sections ( $P = 0.015$ ). All the correlations were confirmed, even after outlier removal, and are reported in supplementary Fig. S1, available at *Rheumatology* Online. No correlations have been observed between molecular and IHC data.

## Discussion

OA is considered to be a whole-joint disease, and it has been suggested that the IFP plays an active role in the OA inflammatory process [19, 20]. Here we observed an increase in lymphocytic infiltration, vascularity and thickness of the interlobular septa of OA IFPs compared with those of controls. Moreover, we evaluated the IFP adjacent synovial membrane histology using the Scanzello histological scoring system [15, 16], showing an increase in lymphocytic infiltration, hyperplasia, vascularity and fibrosis compared with in controls. The presence of mononuclear cell infiltration is consistent with other findings showing similar immune cell composition in the OA IFP and synovial membrane [21]. IHC analysis using anti-MCP-1 and anti-IL-6 showed roundish, isolated positive cells (grade 1) and/or crown-like structures (grade 2) in all OA IFP samples, while positive MCP-1 and IL-6 immunostaining of grade 1 was found only in 20% of the control samples. These crown-like structures have been

previously described in inflamed adipose tissue in people with obesity [22]. They seem to be formed by monocytes/macrophages localized in the periphery of degenerating adipocytes [22, 23]. Recruitment of blood-derived inflammatory cells mediated via different adipokines and forming the crown-like structures might be the source of further inflammatory cytokines and chemokines. Indeed, the higher grades of infiltration observed in EE sections were associated with increased MCP-1 and IL-6 immunostaining detected by IHC.

Vascularity was increased in both OA IFPs and adjacent synovial membranes compared with in controls. Fibrosis represents an ubiquitous tissue response to an unresolved chronic inflammation [17], and the presence of a fibrotic process in the IFPs of OA patients undergoing TKR is not novel [19]. Here, we described an increased thickness of the interlobular septa in the OA IFPs compared with in controls. Furthermore, the OA synovial membrane exhibited fibrosis in 81.9% of patients. Henegar *et al.* [24] demonstrated that in the white adipose tissue of obese subjects there is an increase in the extracellular matrix components, both at the gene expression and protein levels, suggesting that an inflammatory stimulus may be responsible for an excessive synthesis of extracellular matrix components and subsequent interstitial deposition of fibrotic material. The relationship between inflammation and fibrosis is also supported in the present study by the finding that OA patients with lymphocytic infiltration of IFPs had thicker lobuli septa and smaller adipose lobuli compared with controls. In addition, the parallelism

between microscopic changes in the synovial membrane and IFPs might suggest a common pathological process involving both tissues and/or cell–cell cross-talk.

Histological changes such as IFP fibrosis may be involved not only in molecular OA processes, but may also cause an alteration of the IFP biomechanical properties, modifying its ability to absorb gravitational forces acting on the knee joint, and thus promoting and perpetuating joint damage [25].

In addition, we analysed the expression of adipocytokines, correlating them with the histological and molecular features of the OA IFP and the adjacent synovium. Unfortunately, we were not able to compare the mRNA expression levels of OA IFPs with those of the cadavers used as controls, which is a limitation of this study. However, we performed IHC for VEGF, MCP-1 and IL-6 in IFPs of patients affected by OA and also of control patients. In our cohort, no relevant differences were observed with respect to the presence of lymphocytic infiltration after grouping OA patients according to BMI.

Surprisingly, we observed a positive correlation between the expression of adiponectin and leptin mRNA levels in OA IFPs. Moreover, both adipokines were correlated with MCP-1 mRNA levels, and adiponectin was correlated with PPAR $\gamma$  mRNA levels. Classically, leptin and adiponectin, both produced by white adipocytes, are considered to be pro-inflammatory and anti-inflammatory adipokines, respectively [26]. However, the relationship between inflammation and these two adipokines within joints remains controversial. In fact, there are some studies supporting a pro-inflammatory role and others suggesting an anti-inflammatory action of these two proteins [27–34].

In support of our findings, a recent study suggested that adiponectin might have a pro-inflammatory role in IFP tissue, inducing the expression of inflammatory markers in chondrocyte cell lines [31]. Francin *et al.* [30] demonstrated that adiponectin stimulated MMP-13 and PGE2 expression in chondrocytes. Moreover, a pro-inflammatory role of adiponectin was demonstrated in human synovial fibroblasts, inducing the expression of several MMPs [32]. It is likely that the different actions of adiponectin might be related to the existence of the following adiponectin isoforms: low-molecular-weight (LMW) trimer, medium-molecular-weight (MMW) hexamer and high-molecular-weight (HMW) multimer. It has been shown that only LMW adiponectin displays anti-inflammatory properties *in vitro*, while MMW and HMW adiponectin exhibit pro-inflammatory properties *in vitro* [35, 36]. On the other hand, leptin has been shown to increase the expression of several metalloproteinases (MMPs), a disintegrin and metalloproteinase with thrombospondin motifs - 4 (ADAMTS-4) and ADAMTS-5 in rat cartilage [27], and the secretion of inflammatory molecules such as IL-6 and IL-8 in human OA cartilage [33]. In the light of these studies, the positive correlation between adiponectin and leptin in OA IFPs might suggest a synergistic pro-inflammatory action in knee OA, supported also by the direct correlation of both adipokines with MCP-1 expression. Nevertheless,

an association between molecular and immunohistochemical data has not been found.

PPAR $\gamma$ , a regulator of glucose and lipids metabolism, is well known as an inducer of adiponectin expression in adipocytes, supporting the correlation observed here [14]. Nevertheless, an anti-inflammatory role of PPAR $\gamma$  in OA cartilage has been described [37]. However, no studies have analysed the relationship between PPAR $\gamma$  and MCP-1 in OA; thus the role of PPAR $\gamma$  in the setting of inflammation remains controversial. We showed a strong positive correlation between MCP-1 and PPAR $\gamma$  expression levels. Adiponectin has been shown to induce *in vitro* angiogenesis in endothelial cells [38], supporting the positive correlation observed here between adiponectin expression levels and the number of blood vessels in OA IFPs. In addition, IFP VEGF expression levels were associated with increased synovial vascularity, suggesting a possible interaction between the IFP and the adjacent synovial membrane.

It is known that IL-6 is increased in OA IFPs in comparison with the subcutaneous adipose tissue, suggesting a pro-inflammatory role of the IFP in the pathogenesis of OA [9]. We have shown that OA IFP lobules dimensions are correlated positively with IL-6 expression, and correlated negatively with the thickness of interlobular septa. Surprisingly, IL-6 expression was not correlated with lymphocytic infiltration of either IFP or synovial membrane. The OA structural changes evidenced by histology were an increase in inflammatory cells, a reduction of adipose tissue, and an increase in fibrosis, changes that could have affected IL-6 expression.

The correlations observed here between gene expression and the histological characteristics underline the potential cross-talk between the IFP and the synovial membrane, and the importance of the histological changes (such as fibrosis) in cytokines production, thus helping our understanding of OA pathology. In addition, the correlations observed between adipokines and cytokines might be useful for identifying novel targets for the development of new pharmacological treatments for this invalidating disease.

The age and BMI of the OA group were significantly different compared with controls, although no relevant differences were found in our study grouping OA patients according to age and BMI. Regarding this point, an abstract has been presented at the 2016 OARSI conference, confirming that BMI does not affect OA IFP adipocytes size [39]. In our study, BMI was correlated only with the thickness of interlobular septa. No associations were found between BMI or age and IFP or synovial membrane lymphocytic infiltration or vascularization. We did not perform a multivariate analysis adjusting for BMI and age because of the small number of patients. Furthermore, the mRNA from cadaver IFPs was not available. Nevertheless, we performed IHC for VEGF, MCP-1 and IL-6.

In conclusion, our study describes for the first time the histopathological characteristics of IFPs in a cohort of patients with knee OA compared with non-OA controls. IFP



showed pathologic structural changes in terms of fibrosis, vascularization and inflammatory infiltrates. Importantly, these changes were also observed in the IFP adjacent synovial membrane, suggesting a possible cross-talk between these two tissues, which needs to be better explored.

## Acknowledgements

The authors are grateful to Dr Maria Martina Sfriso, Dr Alessandro Frigo and Dr Assunta Pozzuoli for their skillful technical assistance. Moreover, they thank Dr Francesca Ometto for statistical advice. Author contributions: conception and design of the study, or acquisition of data or analysis and interpretation of data: M.F., E.H., E.B., M.G., C.I., A.C., A.P., G.S., A.R., C.G.F., A.N., P.R., R.R., R.D.C., R.V., M.R., V.M. Drafting the article or revising it critically for important intellectual content: M.F., E.H., E.B., M.G., C.I., A.P., A.N., P.R., R.V., M.R., V.M. Final approval of the version to be submitted: all authors approved the final version of the manuscript.

**Funding:** This work was supported by PRAT, the University of Padova (CDPA 155521) and partially by a grant from the Italian Ministry of Health (Ricerca Finalizzata-Giovani Ricercatori – project code: GR-2010-2317593).

**Disclosure statement:** The authors have declared no conflicts of interest.

## Supplementary data

Supplementary data are available at *Rheumatology* Online.

## References

- Goldring MB, Goldring SR. Osteoarthritis. *J Cell Physiol* 2007;213:626–34.
- Cross M, Smith E, Hoy D *et al.* The global burden of hip and knee osteoarthritis: estimates from the global burden of disease 2010 study. *Ann Rheum Dis* 2014;73:1323–30.
- Heidari B. Knee osteoarthritis prevalence, risk factors, pathogenesis and features: Part I. *Caspian J Intern Med* 2011;22:205–12.
- Loeser RF, Goldring SR, Scanzello CR, Goldring MB. Osteoarthritis: a disease of the joint as an organ. *Arthritis Rheum* 2012;64:1697–707.
- Goldring MB, Otero M. Inflammation in osteoarthritis. *Curr Opin Rheumatol* 2011;23:471–8.
- Vahlensieck M, Linneborn G, Schild H, Schmidt HM. Hoffa's recess: incidence, morphology and differential diagnosis of the globular-shaped cleft in the infrapatellar fat pad of the knee on MRI and cadaver dissections. *Eur Radiol* 2002;12:90–3.
- Clockaerts S, Bastiaansen-Jenniskens YM, Runhaar J *et al.* The infrapatellar fat pad should be considered as an active osteoarthritic joint tissue: a narrative review. *Osteoarthritis Cartilage* 2010;18:876–82.
- Belluzzi E, El Hadi H, Granzotto M *et al.* Systemic and local adipose tissue in knee osteoarthritis. *J Cell Physiol* 2017;232:1971–8.
- Schäffler A, Ehling A, Neumann E *et al.* Adipocytokines in synovial fluid. *JAMA* 2003;290:1709–10.
- Distel E, Cadoudal T, Durant S *et al.* The infrapatellar fat pad in knee osteoarthritis: an important source of interleukin-6 and its soluble receptor. *Arthritis Rheum* 2009;60:3374–7.
- Klein-Wieringa IR, Kloppenburg M, Bastiaansen-Jenniskens YM *et al.* The infrapatellar fat pad of patients with osteoarthritis has an inflammatory phenotype. *Ann Rheum Dis* 2011;70:851–7.
- Ushiyama T, Chano T, Inoue K, Matsusue Y. Cytokine production in the infrapatellar fat pad: another source of cytokines in knee synovial fluids. *Ann Rheum Dis* 2003;62:108–12.
- Macchi V, Porzionato A, Sarasin G *et al.* The infrapatellar adipose body: a histotopographic study. *Cells Tissues Organs* 2016;201:220–31.
- Ahmadian M, Suh JM, Hah N *et al.* PPAR[gamma] signaling and metabolism: the good, the bad and the future. *Nat Med* 2013;19:557–66.
- Scanzello CR, Albert AS, DiCarlo E *et al.* The influence of synovial inflammation and hyperplasia on symptomatic outcomes up to 2 years post-operatively in patients undergoing partial meniscectomy. *Osteoarthritis Cartilage* 2013;21:1392–9.
- Scanzello CR, McKeon B, Swaim BH *et al.* Synovial inflammation in patients undergoing arthroscopic meniscectomy: molecular characterization and relationship to symptoms. *Arthritis Rheum* 2011;63:391–400.
- Cinti S, Mitchell G, Barbatelli G *et al.* Adipocyte death defines macrophage localization and function in adipose tissue of obese mice and humans. *J Lipid Res* 2005;46:2347–55.
- Pfaffl MW, Tichopad A, Prgomet C, Neuvians TP. Determination of stable housekeeping genes, differentially regulated target genes and sample integrity: BestKeeper-Excel-based tool using pair-wise correlations. *Biotechnol Lett* 2004;26:509–15.
- Macule F, Sastre S, Lasurt S *et al.* Hoffa's fat pad resection in total knee arthroplasty. *Acta Orthop Belg* 2005;71:714–7.
- Eymard F, Pigenet A, Citadelle D *et al.* Knee and hip intra-articular adipose tissues (IAATs) compared with autologous subcutaneous adipose tissue: a specific phenotype for a central player in osteoarthritis. *Ann Rheum Dis* 2017;76:1142–8.
- Klein-Wieringa IR, de Lange-Brokaar BJ, Yusuf E *et al.* Inflammatory cells in patients with endstage knee osteoarthritis: a comparison between the synovium and the infrapatellar fat pad. *J Rheumatol* 2016;43:771–8.
- Murano I, Barbatelli G, Parisani V *et al.* Dead adipocytes, detected as crown-like structures, are prevalent in visceral fat depots of genetically obese mice. *J Lipid Res* 2008;49:1562–8.
- Weisberg SP, McCann D, Desai M *et al.* Obesity is associated with macrophage accumulation in adipose tissue. *J Clin Invest* 2003;112:1796–808.

- 24 Henegar C, Tordjman J, Achard V *et al.* Adipose tissue transcriptomic signature highlights the pathological relevance of extracellular matrix in human obesity. *Genome Biol* 2008;9:R14.
- 25 Clements KM, Ball AD, Jones HB *et al.* Cellular and histopathological changes in the infrapatellar fat pad in the monoiodoacetate model of osteoarthritis pain. *Osteoarthritis Cartilage* 2009;17:805–12.
- 26 Ouchi N, Parker JL, Lugus JJ, Walsh K. Adipokines in inflammation and metabolic disease. *Nat Rev Immunol* 2011;11:85–97.
- 27 Bao JP, Chen WP, Feng J *et al.* Leptin plays a catabolic role on articular cartilage. *Mol Biol Rep* 2010;37:3265–72.
- 28 Chen TH, Chen L, Hsieh MS *et al.* Evidence for a protective role for adiponectin in osteoarthritis. *Biochimica et biophysica Acta* 2006;1762:711–8.
- 29 Dumond H, Presle N, Terlain B *et al.* Evidence for a key role of leptin in osteoarthritis. *Arthritis Rheum* 2003;48:3118–29.
- 30 Francin PJ, Abot A, Guillaume C *et al.* Association between adiponectin and cartilage degradation in human osteoarthritis. *Osteoarthritis Cartilage* 2014;22:519–26.
- 31 Lago R, Gomez R, Otero M *et al.* A new player in cartilage homeostasis: adiponectin induces nitric oxide synthase type II and pro-inflammatory cytokines in chondrocytes. *Osteoarthritis Cartilage* 2008;16:1101–9.
- 32 Tang CH, Chiu YC, Tan TW, Yang RS, Fu WM. Adiponectin enhances IL-6 production in human synovial fibroblast via an AdipoR1 receptor, AMPK, p38, and NF-kappa B pathway. *J Immunol* 2007;179:5483–92.
- 33 Vuolteenaho K, Koskinen A, Kukkonen M *et al.* Leptin enhances synthesis of proinflammatory mediators in human osteoarthritic cartilage—mediator role of NO in leptin-induced PGE2, IL-6, and IL-8 production. *Mediators Inflamm* 2009;2009:345838.
- 34 Yang WH, Liu SC, Tsai CH *et al.* Leptin induces IL-6 expression through OBRI receptor signaling pathway in human synovial fibroblasts. *PLoS One* 2013;8:e75551.
- 35 Neumeier M, Weigert J, Schaffler A *et al.* Different effects of adiponectin isoforms in human monocytic cells. *J Leukoc Biol* 2006;79:803–8.
- 36 Schober F, Neumeier M, Weigert J *et al.* Low molecular weight adiponectin negatively correlates with the waist circumference and monocytic IL-6 release. *Biochem Biophys Res Commun* 2007;361:968–73.
- 37 Fahmi H, Martel-Pelletier J, Pelletier JP, Kapoor M. Peroxisome proliferator-activated receptor gamma in osteoarthritis. *Modern Rheumatol* 2011;21:1–9.
- 38 Ouchi N, Kobayashi H, Kihara S *et al.* Adiponectin stimulates angiogenesis by promoting cross-talk between AMP-activated protein kinase and Akt signaling in endothelial cells. *J Biol Chem* 2004;279:1304–9.
- 39 Garcia J, Wei W, Runhaar J *et al.* Obesity does not affect the size of infrapatellar fat pad adipocytes: implications for the pathogenesis of knee osteoarthritis. *Osteoarthritis Cartilage* 2016;24:S334–S5.